Influence of the Oxidation on the Magnetic and Transport Properties in the $(La_{1-x}Ca_x)_zMn_zO_y$ ($0 < x < 0.3$) System

E. Herrero,[†,‡] J. Alonso,[†,§] J. L. Martínez,[§] M. Vallet-Regí,[†,||] and J. M. González-Calbet*[,†,‡]

Instituto de Magnetismo Aplicado, RENFE-UCM, Apdo. 155, 28230-Las Rozas Madrid. Spain; Dpto. Química Inorgánica, Facultad de Químicas, Universidad Complutense, 28040-Madrid, Spain; Instituto de Ciencia de Materiales de Madrid, CSIC, Cantoblanco, 28049-Madrid, Spain; and Dpto. Química Inorgánica y Bioinorgánica, Facultad de Farmacia, Universidad Complutense, 28040-Madrid, Spain

Received October 21, 1999. Revised Manuscript Received December 28, 1999

Samples of the $La_{1-x}Ca_xMnO_y$ system have been prepared under different atmospheres. Compositional analysis by electron probe microanalysis, atomic absorption, and thermogravimetric analysis reveals that the samples prepared in air show, in all cases, cationic and anionic vacancies which lead to a general composition $(La_{1-x}Ca_x)_zMn_zO_y$, where $z < 1$ and $y < 3$. When these samples are oxidized, z remains constant, and the oxygen content increases up to $y \sim 3$, i.e., until the anionic perovskite sublattice is practically fully occupied. The precise knowledge of both the Mn^{3+}/Mn^{4+} ratio and the oxygen content allows one to assess its influence on the properties. The oxidation of these materials is accompanied by a strong decrease of their resistance; also, an increase in the magnetoresistance takes place, which is especially important at room temperature.

Introduction

The influence of the oxygen content on the structural, magnetic, and electric properties of $LaMnO_{3+\delta}$ has been widely studied. For $\delta = 0$, the material is an orthorhombic, antiferromagnetic insulator with a very strong Jahn−Teller distortion (only Mn^{3+}). For $\delta \geq 0.1$, i.e, for a Mn^{4+} content of around 20%, the material becomes rhombohedral with a ferromagnetic and metallic behavior at temperatures below T_c, also showing giant magnetoresistance (GMR).[1−8] However, it has been stated that $\delta > 0$ does not mean interstitial oxygens are present, but Mn^{3+} transforms into Mn^{4+}, as a consequence of the existence of cationic vacancies[3,8−10] similar in both lattice sites. Consequently, the formulation $La_{1-t}Mn_{1-t}O_3$ ($t = \delta/3 + \delta$) has been proposed, considering that the anionic sublattice is complete.

Such mixed oxidation states can be also obtained by doping with alkaline-earth cations (Ca, Ba, Sr), and depending on the dopant amount, the properties of these systems are also affected. For example, in the $La_{1-x}Ca_xMnO_3$ system, a ferromagnetic and insulating behavior can be observed for $x < 0.2$, whereas for $x \geq 0.2$, i.e., around 20% Mn^{4+}, the system becomes metallic and ferromagnetic and shows GMR.[11]

According to this behavior, it should be expected that if it were possible to oxidize $x < 0.2$ samples up to values of Mn^{4+} around 20%, they will be also metallic−ferromagnetic and highly magnetoresistant. For instance, Mahendiran et al.[12] report samples with $x = 0.1$ and 0.2, prepared by the ceramic method, showing such a behavior. Other authors suggest that the oxidation of $La_{1-x}Ca_xMnO_3$ materials showed no significant variation in their magnetic and electric properties.[10] However, it must be considered that these experiments were carried out under severe oxidation conditions (200 atm of O_2), which lead to high δ values and, consequently, to a high cationic vacancies concentration.[13,14] Since the

[†] Instituto de Magnetismo Aplicado.
[‡] Dpto. Química Inorgánica, Facultad de Químicas, Universidad Complutense.
[§] Instituto de Ciencia de Materiales de Madrid.
[||] Dpto. Química Inorgánica y Bioinorgánica, Facultad de Farmacia, Universidad Complutense.

(1) Wollan, E. O.; Koehler, W. C. *Phys. Rev.* **1955**, *100*, 545.
(2) Elemans, J. B. A. A.; Van Laar, B.; Van der Veen, K. R.; Loopstra, B. O. *J. Solid State Chem.* **1971**, *3*, 238.
(3) Tofield, B. C.; Scott, W. R. *J. Solid State Chem.* **1974**, *10*, 183.
(4) Kamata, K.; Nakajima, T.; Hayashi, T.; Nakamura, T. *Mater. Res. Bull.* **1978**, *13*, 49.
(5) Kuo, J. H.; Anderson, H. U.; Sparlin, D. M. *J. Solid State Chem.* **1990**, *87*, 55.
(6) Takeda, Y.; Nakai, S.; Kojima, T.; Kanno, R.; Imanishi, N.; Shen, G. Q.; Yamamoto, O. *Mater. Res. Bull.* **1991**, *26*, 153.
(7) Verelst, M.; Rangavittal, N.; Rao, C. N. R.; Rousset, A. *J. Solid State Chem.* **1993**, *104*, 74.
(8) Ritter, C.; Ibarra, M. R.; de Teresa, J. M.; Algarabel, P. A.; Marquina, C.; Blasco, J.; García, J.; Oseroff, S.; Cheong, S.-W. *Phy. Rev. B* **1997**, *56*, 8902.
(9) Van Roosmalen, J. A. M.; Cordfunke, E. H. P.; Helmholdt, R. B.; Zandbergen, H. W. *J. Solid State Chem.* **1994**, *110*, 100.
(10) Hervieu, M.; Mahesh, R.; Rangavittal, N.; Rao, C. N. R. *Eur. J. Solid State Inorg. Chem.* **1995**, *32*, 79
(11) Schiffer, P.; Ramirez, A. P.; Bao, W.; Cheong, S. W. *Phys. Rev. Lett.* **1995**, *75*, 3336.
(12) Mahendiran, R.; Tiwary, S. K.; Raychaudhuri, A. K.; Ramakrishnan, T. V.; Mahesh, R.; Rangavittal, N.; Rao, C. N. R. *Phys. Rev. B* **1996**, *53*, 3348.
(13) Alonso, J. A.; Martínez-Lope, M. J.; Casais, M. T.; MacManus-Driscoll, J. L.; de Silva, P. S. I. P. N.; Cohen, L. F.; Fernández-Díaz, M. T. *J. Mater. Chem.* **1997**, *7*, 2139.
(14) Alonso, J. A.; Martínez-Lope, M. J.; Casais, M. T.; Muñoz, A. *Solid State Commun.* **1997**, *102*, 7.

10.1021/cm9911619 CCC: $19.00
Published on Web 03/15/2000

appearance of ferromagnetic and metallic behavior in these samples is due to the double-exchange behavior of $Mn^{3+}-O-Mn^{4+}$, the presence of a high number of vacancies does not favor this phenomenon. It can be concluded that strong oxidation conditions do not seem the most appropriate to obtain metallic behavior and GMR effect in these type of manganites. In fact, Dabrowski et al.[15] have very recently shown that it is possible to modify δ in $La_{0.74}Ca_{0.26}MnO_{3+\delta}$, by varying the synthesis conditions, with T_c increasing when the oxygen content increases. However, when such a material is treated under high oxygen pressure (12 and 140 atm O_2), T_c decreases.

This work deals with the oxidation, under soft conditions, of $La_{1-x}Ca_xMnO_3$ ($0.05 < x < 0.33$), focusing on the determination, as accurately as possible, of the cationic ratio (La−Ca−Mn), the oxygen content, and the manganese oxidation state, to correlate them to the possible variation of their magnetic and transport properties, as well as the structural transitions that will occur in the oxidized samples.

Experimental Section

The samples prepared in air (A_x samples, where $x = 0.05$, 0.1, 0.2, 0.25, 0.33) were synthesized by the ceramic method. Stoichiometric amounts of La_2O_3, $CaCO_3$, and MnO_2 were homogenized and milled in an agate mill and heated at 1400 °C for 110 h, with several intermediate grindings. The samples were finally quenched to room temperature.

The oxidized samples (O_x samples) were obtained by annealing the samples prepared in air at 1300 °C for 24 h under an oxygen flow. These materials were cooled (2 °C/min) to room temperature inside the furnace under oxygen flow.

The Mn content was determined by atomic absorption technique in a Perkin Elmer 11003, while the La, Ca and Mn ratios were determined by means of an electron probe microanalyzer (EPMA), attached to a JEOL JXA-8900M microscope. The oxygen content was determined by thermogravimetric analysis in a Cahn D-200 electrobalance. X-ray diffraction (XRD) was carried out in a Siemens D-5000 diffractometer (Cu Kα). Selected area electron diffraction (SAED) and transmission electron microscopy (TEM) were performed in a JEOL 2000 FX electron microscope. The magnetic susceptibility was measured in a SQUID (MPMS-5S Quantum Design, San Diego) magnetometer, with a temperature range between 4 and 400 K and an applied field of 0.1 T. The resistance measurements were carried out by the four contacts method by means of PPMS (Quantum Design) with fields of 0 to 9 T and temperature interval from 5 to 400 K.

Results

In this paper, we report a statistical study of composition and homogeneity of all samples. At least 12 different crystals in each sample were examined. The results obtained for the nominal composition $La_{0.95}Ca_{0.05}MnO_y$ are shown in Table 1.Since we also checked by atomic absorption the total content of manganese, finding that the theoretical value agrees in all cases with the experimental value, it is possible to normalize the percent mole values of manganese and to obtain the composition for every crystal. As it can be seen, the sample is very homogeneous, there are no compositional differences between different crystals or inside a single crystal. The nominal composition of this material is always within the deviation limits for each analyzed crystal.

Table 1. Microprobe Analysis of the Sample with Nominal Composition $La_{0.95}Ca_{0.05}MnO_y$

crystal	La % mol	Ca % mol	Mn % mol	composition
1	41.7	1.5	44.0	$La_{0.95}Ca_{0.03}MnO_y$
2	40.5	2.1	44.0	$La_{0.92}Ca_{0.05}MnO_y$
3	41.8	1.8	43.7	$La_{0.96}Ca_{0.04}MnO_y$
4	41.8	1.2	44.3	$La_{0.954}Ca_{0.03}MnO_y$
5	41.2	1.7	43.6	$La_{0.94}Ca_{0.04}MnO_y$
6	41.0	2.2	43.5	$La_{0.94}Ca_{0.05}MnO_y$
7	41.3	2.5	44.8	$La_{0.92}Ca_{0.06}MnO_y$
8	41.8	1.6	44.2	$La_{0.95}Ca_{0.04}MnO_y$
9	41.3	2.0	43.3	$La_{0.95}Ca_{0.05}MnO_y$
10	41.3	1.9	44.5	$La_{0.93}Ca_{0.04}MnO_y$
11	41.8	1.0	44.6	$La_{0.94}Ca_{0.02}MnO_y$
12	41.8	1.3	44.0	$La_{0.95}Ca_{0.03}MnO_y$
av.	41.4	1.7	44.0	$La_{0.94(2)}Ca_{0.04(2)}MnO_y$

Table 2. Final Microprobe Analysis Results of $La_{1-x}Ca_xMnO_y$ Samples

sample	La % mol	Ca % mol	Mn % mol	composition
$A_{0.05}$	41.4	1.7	44.0	$La_{0.94(2)}Ca_{0.04(2)}MnO_y$
$A_{0.10}$	40.0	3.8	45.0	$La_{0.89(2)}Ca_{0.08(3)}MnO_y$
$A_{0.20}$	37.3	9.2	46.4	$La_{0.80(2)}Ca_{0.20(1)}MnO_y$
$A_{0.25}$	36.1	11.3	46.9	$La_{0.77(3)}Ca_{0.24(2)}MnO_y$
$A_{0.33}$	31.15	15.3	46.5	$La_{0.67(2)}Ca_{0.33(2)}MnO_y$

Table 3. Chemical Composition of $La_{1-x}Ca_xMnO_y$ Samples

sample	% Mn^{4+}	composition
$A_{0.05}$	9	$(La_{0.95}Ca_{0.05})_{0.96}$ $(Mn^{4+}_{0.09}Mn^{3+}_{0.91})_{0.96}O_{2.90}$
$A_{0.10}$	14	$(La_{0.90}Ca_{0.10})_{0.97}$ $(Mn^{4+}_{0.14}Mn^{3+}_{0.86})_{0.97}O_{2.93}$
$A_{0.20}$	24	$(La_{0.80}Ca_{0.20})_{0.99}$ $(Mn^{4+}_{0.24}Mn^{3+}_{0.76})_{0.99}O_{2.98}$
$A_{0.25}$	25	$(La_{0.75}Ca_{0.25})_{0.99}$ $(Mn^{4+}_{0.25}Mn^{3+}_{0.75})_{0.99}O_{2.99}$
$O_{0.05}$	27	$(La_{0.95}Ca_{0.05})_{0.96}(Mn^{4+}_{0.27}Mn^{3+}_{0.73})_{0.96}O_3$
$O_{0.10}$	28	$(La_{0.90}Ca_{0.10})_{0.97}(Mn^{4+}_{0.28}Mn^{3+}_{0.72})_{0.97}O_3$
$O_{0.20}$	28	$(La_{0.80}Ca_{0.20})_{0.99}(Mn^{4+}_{0.28}Mn^{3+}_{0.72})_{0.99}O_3$
$O_{0.25}$	27	$(La_{0.75}Ca_{0.25})_{0.99}(Mn^{4+}_{0.27}Mn^{3+}_{0.73})_{0.99}O_3$

Similar results were obtained for all samples. Table 2 shows the average composition of all samples under study. Since the nominal compositions are always within the compositional error limits for each sample, from now on we will always refer to nominal composition, keeping in mind the experimental errors. The oxidized samples present the same cationic composition as the air samples.

The oxygen content was determined by thermogravimetric analysis; this technique allows also to determine indirectly the Mn^{4+} content in each sample, because the oxidation states of lanthanum (3+) and calcium (2+) remain constant. The results obtained in both air and oxidized samples are shown in Table 3. As can be observed, for A_x materials, the Mn^{4+} content increases with the calcium content, being slightly higher than the corresponding calcium content.

The thermogravimetric analysis of oxidized samples O_x shows that all samples present an increase in the oxygen content which is smaller for higher Ca contents. This is clearly observed by comparing the thermogravimetric curves of a sample with the same cationic ratio but under different atmospheres. Thus, Figure 1 shows the results for $A_{0.05}$ and $O_{0.05}$ materials. It seems clear that the oxidized sample loses more weight than the sample prepared in air. Since the cationic composition is the same and does not vary during the oxidation process $A_{0.05} \rightarrow O_{0.05}$, as demonstrated by chemical

(15) Dabrowski, B.; Klamut, P. W.; Bukowski, Z.; Dybzinski, R.; Siewenie, J. E. *J. Solid State Chem.* **1999**, *144*, 461.

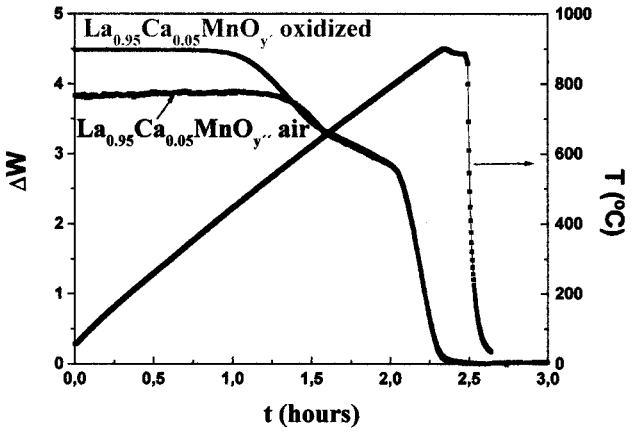

Figure 1. TGA curves corresponding to the $A_{0.05}$ and $O_{0.05}$ samples.

analysis, the weight increase can only be due to an increase of the oxygen content. Several authors have stated that no interstitial oxygen is present in these materials.[3,9] Therefore, if this is true, the only explanation to justify the oxidation process $A_{0.05} \rightarrow O_{0.05}$ will be the presence of anionic vacancies in $A_{0.05}$. This increase of the oxygen content is only observed in the range $0 \leq x \leq 0.25$ where all of the O_x samples show a Mn^{4+} content of around 28%. It is worth recalling than the same Mn^{4+} value has been reported for undoped "$LaMnO_{3+\delta}$". It is then possible to assume that the anionic sublattice is complete for around 28% Mn^{4+}.

To justify a $O_{0.05}$ material with the anionic sublattice complete and 28% Mn^{4+}, a small amount of cationic vacancies is necessary. Obviously, the $A_{0.05}$ sample presents the same amount of vacancies, and therefore, the most correct formulation for these materials should be $(La_{0.95}Ca_{0.05})_zMn_zO_{y'}$ for $O_{0.05}$ and $(La_{0.95}Ca_{0.05})_z$-$Mn_zO_{y''}$ for $A_{0.05}$, with z being the same for both samples.

The reduction process (Figure 1) of samples $O_{0.05}$ and $A_{0.05}$ is

$$[O_{0.05}](La_{0.95}Ca_{0.05})_zMn_zO_{y'} \rightarrow \frac{(0.95z)}{2}La_2O_3 + (0.05z)CaO + zMnO$$

$$[A_{0.05}](La_{0.95}Ca_{0.05})_zMn_zO_{y''} \rightarrow \frac{(0.95z)}{2}La_2O_3 + (0.05z)CaO + zMnO$$

From the weight loss, it can be deduced that

$$y' = 3.11z$$

$$y'' = 3.02z$$

If we assume that the most oxidized sample ($O_{0.05}$) has the anionic sublattice complete, without interstitial oxygen, then $y' = 3.0$, and therefore, $z = 0.965$ and $y'' = 2.914$, with the formulations corresponding to $O_{0.05}$ and $A_{0.05}$ being $(La_{0.95}Ca_{0.05})_{0.96}Mn_{0.96}O_{3.0}$ and $(La_{0.95}$-$Ca_{0.05})_{0.96}Mn_{0.96}O_{2.91}$, respectively.

Following the same procedure, we have determined the oxygen content and Mn^{4+} percentage for all of the samples gathered in Table 3. The total amount of cationic vacancies per unit formula is relatively small and decreases as x increases. This small amount justifies that chemical analysis by atomic absorption spectroscopy suggests that the cationic composition is approximately the nominal composition since the difference is included inside the experimental error limit.

Table 4. Lattice Parameters Corresponding to A_x and O_x Materials

sample	*a* (Å)	*b* (Å)	*c* (Å)	composition
$A_{0.05}$	5.600	5.519	7.715	$(La_{0.95}Ca_{0.05})_{0.96}Mn_{0.96}O_{2.90}$
$A_{0.10}$	5.577	5.515	7.748	$(La_{0.90}Ca_{0.10})_{0.97}Mn_{0.97}O_{2.93}$
$A_{0.20}$	5.487	5.488	7.766	$(La_{0.80}Ca_{0.20})_{0.99}Mn_{0.99}O_{2.98}$
$A_{0.25}$	5.472	5.473	7.766	$(La_{0.75}Ca_{0.25})_{0.99}Mn_{0.99}O_{2.99}$
$O_{0.05}$	5.512	5.512	13.36	$(La_{0.95}Ca_{0.05})_{0.96}Mn_{0.96}O_3$
$O_{0.10}$				$(La_{0.90}Ca_{0.10})_{0.97}Mn_{0.97}O_3$
$O_{0.20}$	5.483	5.476	7.738	$(La_{0.80}Ca_{0.20})_{0.99}Mn_{0.99}O_3$
$O_{0.25}$	5.458	5.454	7.734	$(La_{0.75}Ca_{0.25})_{0.99}Mn_{0.99}O_3$

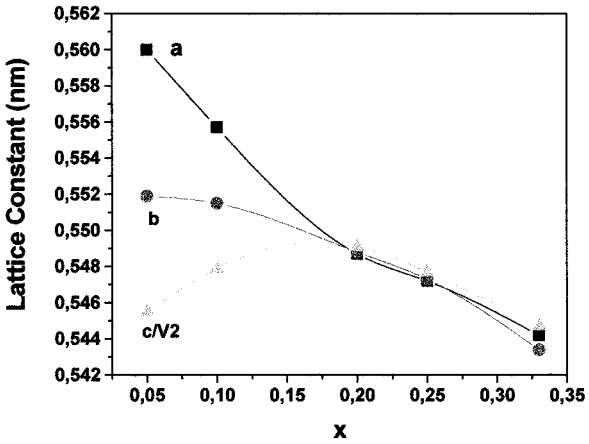

Figure 2. Variation of lattice parameters as a function of Ca content in air-prepared samples.

It seems obvious that in order to compare physical properties as a function of the oxygen content, samples with the same cationic ratio must be used. Besides, the formula up to now accepted for samples with apparent oxygen excess (δ), $La_{1-t}Mn_{1-t}O_3$, with $t = \delta/(3 + \delta)$, seems to be inappropriate, since it can be thought that samples with different δ present identical anionic composition but different cationic ratio.

Initially, the structural characterization of the powder samples was done by XRD. All samples A_x exhibit diffraction patterns characteristic of an orthorhombic symmetry and space group *Pnma*. The lattice parameters of A_x materials are collected in Table 4. The variation of the lattice parameters against x is shown in Figure 2; when x increases, the distortion of lattice parameters decreases, so that for $x = 0.2$, $a \approx b \approx c/(2)^{1/2}$.

The SAED and HREM study (Figure 3a,b) shows that samples exhibit orthorhombic symmetry, all of them being twinned. However, a small number of crystals (less than 5%) with diffraction patterns corresponding to a rhombohedral symmetry and space group $R\bar{3}c$, is found in sample $A_{0.05}$.

In the case of the oxidized samples, the XRD study (Figure 4) shows that for $x = 0.05$ a structural variation from orthorhombic ($a = 5.600$, $b = 5.519$, and $c = 7.715$ Å) to rhombohedral symmetry ($a = 5.520$ and $c = 13.360$ Å) has been produced, as previously observed for $LaMnO_y$[5] and $La_{1-x}Sr_xMnO_3$.[16] Materials with higher oxygen content show rhombohedral symmetry and space group $R\bar{3}c$, whereas those with less oxygen content have

(16) Mitchell, J. F.; Argyriou, D. N.; Potter, C. D.; Hinks, D. G.; Jorgensen, J. D.; Bader, S. D. *Phys. Rev. B.* **1996**, *54*, 6172.

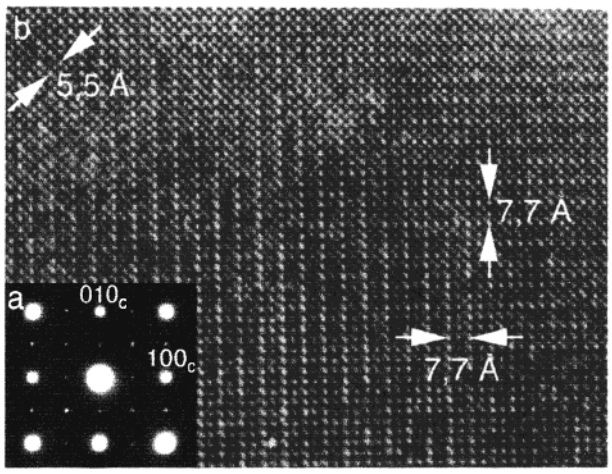

Figure 3. (a) SAED pattern and (b) HREM image corresponding to the $A_{0.20}$ sample along the $[001]_c$ direction. Three-dimensional twinning is clearly observed.

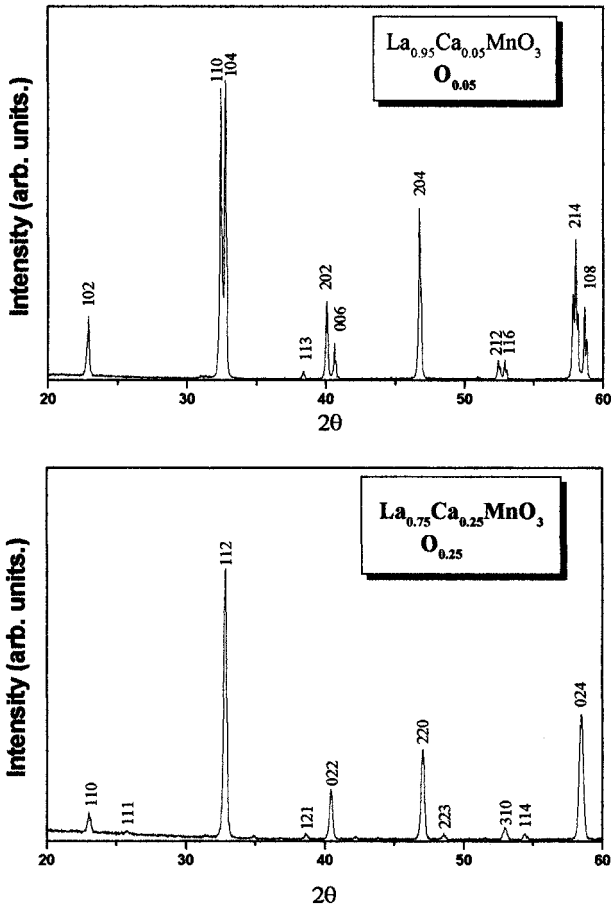

Figure 4. Power XRD patterns of oxidized samples: $O_{0.05}$ and $O_{0.25}$.

orthorhombic symmetry and space group *Pnma*. For $x = 0.25$, no structural transition has been observed, so that the increase of oxygen content in the oxidized samples with respect to air samples is lower. However, the lattice parameters ($a = 5.458$, $b = 5.454$, and $c = 7.734$ Å) are slightly smaller than those of the sample prepared in air, originating a slight contraction of the lattice, probably due to the slight increase in Mn^{4+}. Finally, for $x = 0.10$ and 0.20, the materials show diffraction patterns in which, together with diffraction maxima which can be assigned to an orthorhombic

Table 5. Curie Temperature (T_c), Slope Change of Resistance (T^*), Maximum of Resistance (T_R), Maximum of Magnetoresistance (T_{MR}) Corresponding to Both A_x and O_x Samples

sample	T_c	T^*	T_R	T_{MR}	sample	T_c	T^*	T_R	T_{MR}
$A_{0.05}$	188			179	$O_{0.05}$	180	177	187	170
$A_{0.1}$	195	160	189	185	$O_{0.1}$	183	166	184	186
$A_{0.2}$	208		205	197	$O_{0.2}$	222		226	224
$A_{0.25}$	220		216	210	$O_{0.25}$	240		244	242

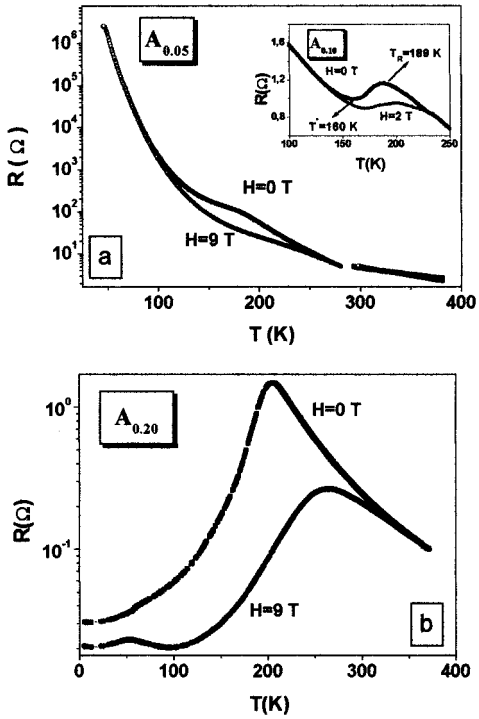

Figure 5. Variation of the resistance as a function of the temperature corresponding to the (a) $A_{0.05}$ and $A_{0.10}$ (inset) samples and the (b) $A_{0.20}$ material.

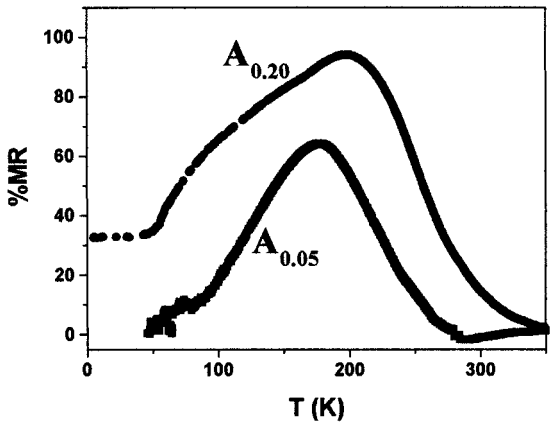

Figure 6. Temperature dependence of the magnetoresistance (R(H=0)−R(H)/R(H=0)) for the $A_{0.05}$ and $A_{0.20}$ samples.

symmetry and space group *Pnma*, appear other maxima that can be attributed to a minority phase with rhombohedral symmetry. This fact suggests that for these materials the oxidation procedure can be heterogeneous leading to the production of crystals with different oxygen content in such a way that crystals with higher oxygen content show rhombohedral symmetry, whereas orthorhombic symmetry is shown by crystals with lower oxygen stoichiometry.

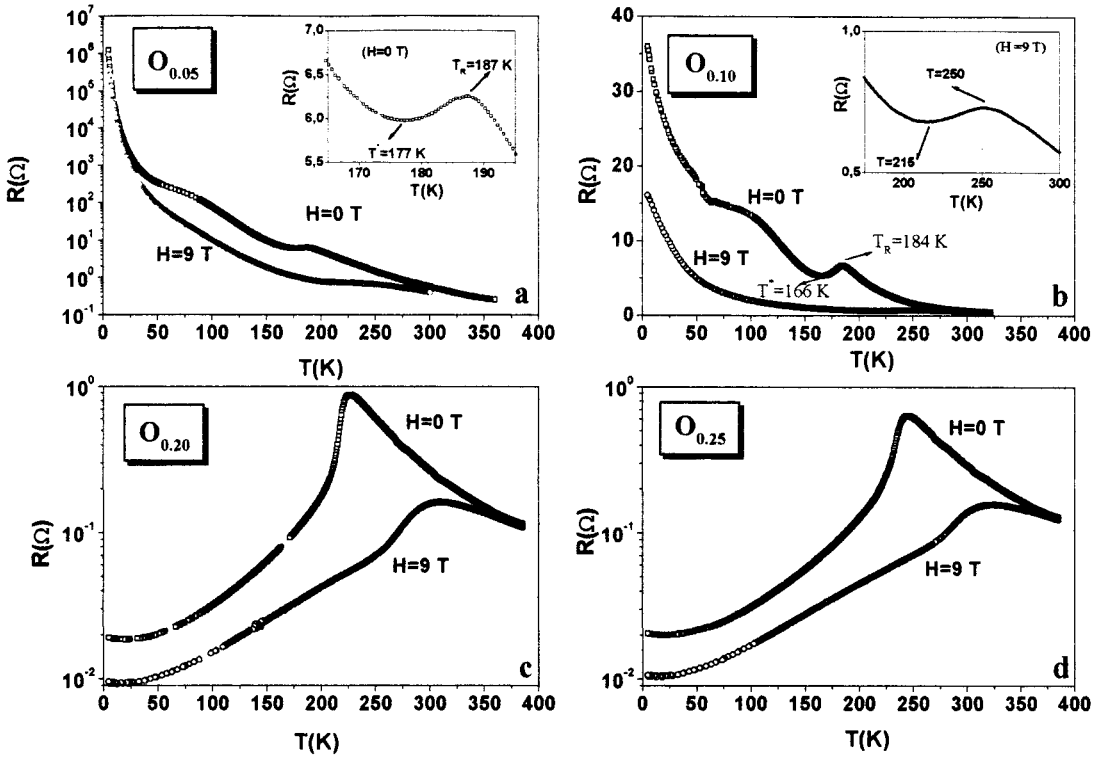

Figure 7. Variation of the resistance as a function of the temperature for oxidized samples (a) $O_{0.05}$, (b) $O_{0.10}$, (c) $O_{0.20}$, and (d) $O_{0.25}$. It is worth recalling that according to XRD patterns the $O_{0.10}$ sample is a mixture of the orthorhombic (∼75%) and rhombohedral (∼25%) phases whereas the $O_{0.20}$ material includes less than 5% of the rhombohedral phase.

The magnetization measurements performed on these materials prepared in air show that all of them exhibit a ferromagnetic behavior (Table 5), with T_c values increasing with the calcium content. Although all of the A_x samples show ferromagnetic behavior, the electrical behavior varies according to the x value. The samples with $x \leq 0.1$ exhibit semiconductor behavior, whereas for $x \geq 0.2$ the materials present a metallic behavior for $T < T_c$.

Figure 5 shows the variation of the resistance of $A_{0.05}$ with temperature. As can be observed at $H = 9$ T, $A_{0.05}$ behaves as a semiconductor throughout the temperature range (Figure 5a). However, for $H = 0$ T, the resistance presents an anomaly near T_c ($T_c \approx 188$ K). For the material $A_{0.10}$, this anomaly consists of the appearance of a minimum in the resistance curve to $T^* = 160$ K, which increases by applying a magnetic field. Therefore, in a relatively narrow temperature range (189−160 K), the sample is metallic and a semiconductor from 160 K. A similar behavior has been observed in $La_{1-x}Sr_xMnO_y$ ($0.1 \leq x \leq 0.15$).[17−19]

The different behavior shown by the resistance of these materials with and without applied field means that, despite their semiconductor behavior, both exhibit noticeable magnetoresistance values that, for sample $A_{0.05}$, reaches 60% (Figure 6). For $x \geq 0.2$, the samples present a metallic behavior from T_c and a remarkable decrease of the resistance upon applying a field of 9 T (Figure 5 b). In this composition interval, the samples possess a magnetoresistance value close to 95% (Figure 6).

The oxidized materials continue being ferromagnetic, but, while for the materials $O_{0.05}$ and $O_{0.10}$ a decrease of T_c takes place (Table 5), for materials $O_{0.20}$ and $O_{0.25}$, T_c increases. The resistance of samples O_x, as well as the material A_x, shows a different behavior with temperature as a function of x. As in the previous case, for $x \leq 0.1$ the materials are, in general, semiconductors, but now the samples $O_{0.05}$ and $O_{0.10}$ also present a minimal in the resistance curve, which can be observed in Figure 7 a,b. For both materials, T^* increases when a magnetic field is applied (Figure 7b). For $x \geq 0.2$ values (Figure 7c,d), the materials keep showing a metallic behavior with a shift of the resistance maximum toward higher temperatures. For all values of x, a remarkable decrease of the resistance takes place under an applied magnetic field, causing high values of magnetoresistance for all samples (see Figure 8.) Besides the fact that a minimum appears in the temperature dependence of the resistivity, the main magnetic behavior (ferromagnetism) is similar in samples with $x = 0.1$ and 0.25 (Figure 9), except for a shift in T_c, but a drop in the magnetic signal is not present, as would be expected for a charge ordering. The signature of the charge localization in magnetic susceptibility is very well understood in the case of $x = 1/2$ and $2/3$, so that a metallic behavior is observed between the long-range ferromagnetic ordering (T_c) and T^*, where some type of charge localization is taking place. For $T < T^*$, the semiconducting behavior appears, but the sample keeps the ferromagnetic behavior.

(17) Urushibara, A.; Moritomo, Y.; Arima, T.; Asamitsu, A.; Kido, G.; Tokura, Y. *Phys. Rev. B* **1995**, *51*, 14103.
(18) Pinsard, L.; Rodríguez-Carvajal, J.; Moudden, A. H.; Anane, A.; Revcolevschi, A.; Dupas, C. *Physica B* **1997**, *234−236*, 856.
(19) Senis, R.; Laukhin, V.; Martínez, B.; Fontcuberta, J.; Obradors, X.; Arsenov, A. A.; Mukovskii, Y. M. *Phys. Rev. B* **1998**, *57*, 14680.

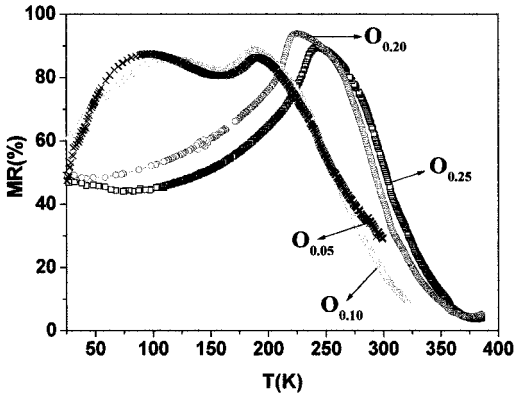

Figure 8. Dependence on temperature of the magnetoresistance percentage of oxidized samples.

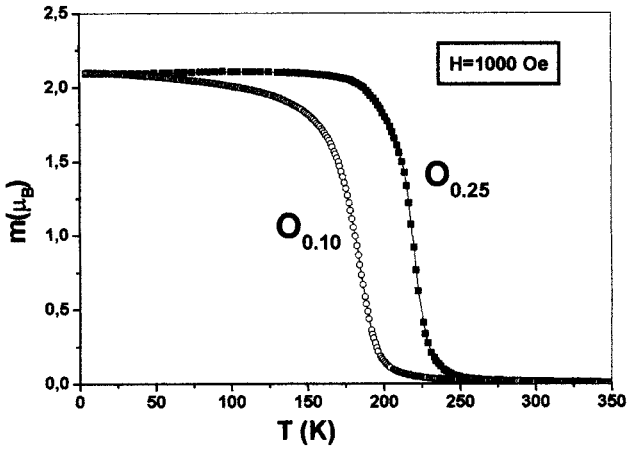

Figure 9. Temperature dependence of the magnetic susceptiblility for the $O_{0.10}$ and $O_{0.25}$ samples.

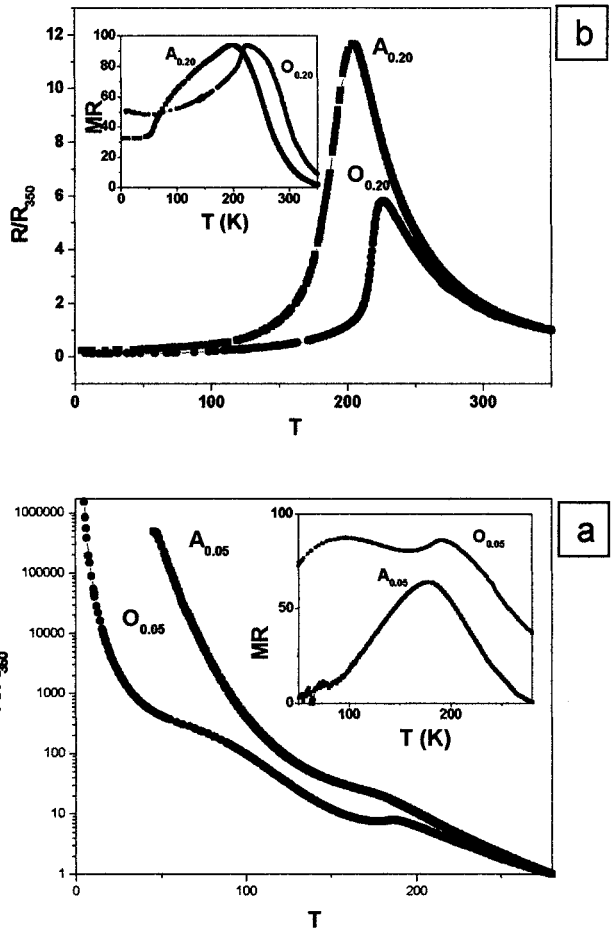

Figure 10. Comparison of the temperature dependence of the normalized resistance and magnetoresistance percentage in air and oxidized samples: (a) $A_{0.05}$ and $O_{0.05}$, and (b) $A_{0.25}$ and $O_{0.25}$.

Discussion

Under the indicated synthesis conditions, the oxidation of the system $La_{1-x}Ca_xMnO_y$ is possible up to a value of $x \approx 0.25$. The materials prepared in air have crystalline structure and electrical and magnetic behaviors similar to those indicated in the literature.

The oxidation of these materials with $x \leq 0.2$ leads to structural variations, giving rise to the appearance of a rhombohedral symmetry, which was not present in the samples prepared in air, except in $A_{0.05}$, in which it appears in a very minor way. On the other hand, the oxidation of the materials is accompanied by a strong decrease of their resistance, as can be observed in Figure 10, which shows the variation of the resistance with the temperature for the materials $La_{0.95}Ca_{0.05}MnO_y$ (Figure 10a) and $La_{0.80}Ca_{0.20}MnO_y$ (Figure 10b) before and after oxidation. In addition, an increase in the magnetoresistance takes place, which is especially important at room temperature because, as can be seen in the inset of Figure 10, the magnetoresistance at ambient temperature of the material $La_{0.80}Ca_{0.20}MnO_y$ goes from 15% before oxidizing to 43% after the oxidation. Another interesting fact is the increase in the T_{MR} (magnetoresistance maximum value) with the oxygen content.

Finally, the most original aspect of the oxidized materials is that, having all of them the same Mn^{4+} content (27−28%), which is the optimum value for the appearance of a metallic behavior, only the materials $O_{0.20}$ and $O_{0.25}$ show such behavior, and they were already metallic before their oxidation. Therefore, it seems that for samples with low calcium content the oxidation does not give rise to significant variations in the transport properties, although the Mn^{4+} content is adequate to produce the exchange phenomena Mn^{3+}−O−Mn^{4+}. It could be thought that this is due to the existence of cationic vacancies in these materials; however, the number of vacancies in the oxidized sample (3.5% for the sample $O_{0.05}$ and 3% for sample $O_{0.10}$) is not high enough to cancel the exchange interaction nor to preclude the percolation paths to produce metallic conductivity. Similarly, the crystalline structure of the material cannot be the cause, because $La_{0.96}Mn_{0.96}O_3$ is rhombohedral,[12] while $La_{0.8}Ca_{0.2}MnO_{3.04}$ is orthorhombic, and both present metallic behavior.

The fact that these materials with high Mn^{4+} content show semiconductor behavior seems to be due, as in the La−Sr−MnO system,[16,17] to an effect of charge localization in connection with the calcium positions. If we assume that Ca is homogeneously distributed along the crystal and Mn^{4+} is localized around a Ca site, the most homogeneous structural model (compatible with the magnetic and structural models proposed by other authors)[1,20] that justifies a metallic behavior is that depicted in Figure 11, corresponding to the $A_{0.25}$ and

(20) Yamada, Y.; Hino, O.; Nohdo, S.; Kanao, R.; Inami, T.; Katano, R. *Phys. Rev. Lett.* **1996**, *77*, 904.

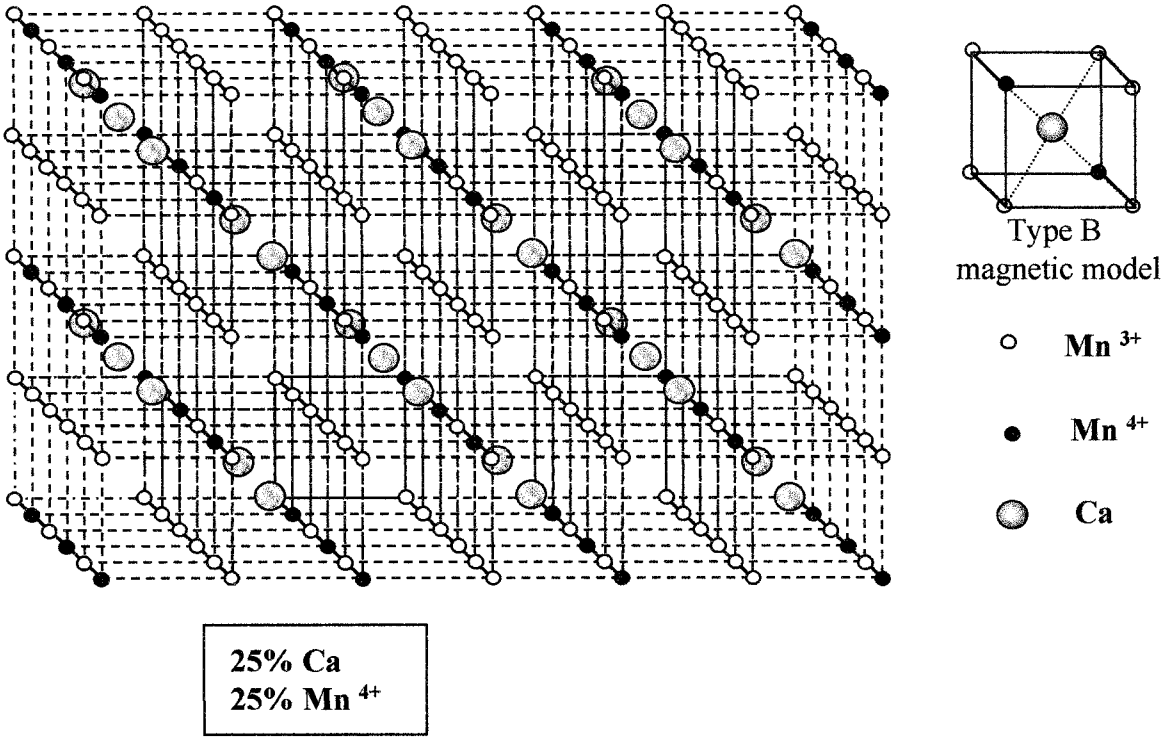

Figure 11. Schematic structural model corresponding to 25% Ca and 25% Mn^{4+}. To better visualize the $Mn^{3+}-O-Mn^{4+}$ sequence and the relative position of Mn^{4+} with respect to calcium, La^{3+}, and oxygen are not included.

$O_{0.25}$ samples. A stacking sequence of $Mn^{3+}-O-Mn^{4+}$ along the three space directions is clearly observed, thus allowing the double exchange while keeping Mn^{4+} in the coordination polyhedra around Ca. This means that a net shifting of the charge along the lattice can occur, without breaking its association with a given Ca atom; therefore, such material would exhibit a metallic behavior.

For samples with lower Ca and Mn^{4+} contents, the situation becomes different. Because of the low Mn^{4+} concentration, a $Mn^{3+}-O-Mn^{4+}$ sequence along the three space directions is not possible. Moreover, the material becomes insulator since charge movement is not possible because it is localized around Ca positions. When such a material is oxidized, the new Mn^{4+} created is placed around calcium sites not forming a sequence of $Mn^{3+}-O-Mn^{4+}$. Therefore, the net shifting does not occur, thus leading to an insulator sample such as the $O_{0.05}$ sample.

According to that, we can conclude that the metallic behavior is associated with the Ca content. For $x \leq 0.1$, samples are insulator whatever the Mn^{4+} content.

Acknowledgment. Financial support through Research Project MAT98-0648 is acknowledged.

CM9911619